Senescence-associated changes in respiration and oxidative phosphorylation in primary human fibroblasts

Eveline HUTTER*[1], Kathrin RENNER†[1], Gerald PFISTER*, Petra STÖCKL*, Pidder JANSEN-DÜRR* and Erich GNAIGER‡[2]

*Abteilung Molekular- und Zellbiologie, Institut für Biomedizinische Alternsforschung der Österreichischen Akademie der Wissenschaften, Rennweg 10, A-6020 Innsbruck, Austria, †Institut für Pathophysiologie, Universität Innsbruck, Fritz-Pregl Str. 3, A-6020 Innsbruck, Austria, and ‡D. Swarovski Research Laboratory, Department of Transplant Surgery, University Hospital Innsbruck, Innrain 66/6, A-6020 Innsbruck, Austria

Limitation of lifespan in replicative senescence is related to oxidative stress, which is probably both the cause and consequence of impaired mitochondrial respiratory function. The respiration of senescent human diploid fibroblasts was analysed by high-resolution respirometry. To rule out cell-cycle effects, proliferating and growth-arrested young fibroblasts were used as controls. Uncoupled respiration, as normalized to citrate synthase activity, remained unchanged, reflecting a constant capacity of the respiratory chain. Oligomycin-inhibited respiration, however, was significantly increased in mitochondria of senescent cells, indicating a lower coupling of electron transport with phosphorylation. In contrast, growth-arrested young fibroblasts exhibited a higher coupling state compared with proliferating controls. In intact cells, partial uncoupling may lead to either decreased oxidative ATP production or a compensatory increase in routine respiration. To distinguish between these alternatives, we subtracted oligomycin-inhibited respiration from routine respiration, which allowed us to determine the part of respiratory activity coupled with ATP production. Despite substantial differences in the respiratory control ratio, ranging from 4 to 11 in the different experimental groups, a fixed proportion of respiratory capacity was maintained for coupled oxidative phosphorylation in all the experimental groups. This finding indicates that the senescent cells fully compensate for increased proton leakage by enhanced electron-transport activity in the routine state. These results provide a new insight into age-associated defects in mitochondrial function and compensatory mechanisms in intact cells.

Key words: aging, coupling state, mitochondria, oxidative stress, primary human fibroblast, respiration, senescence.

INTRODUCTION

Mitochondria have been proposed to be an important link between the age-related accumulation of oxidative damage and the alterations of physiological function associated with aging (see [1] for a review). The free radical theory of aging, which was first proposed by Harman [2], predicts that oxidative damage accumulates in cells and tissues over time and contributes to the decrease in physiological functions with age. This is most evident for tissues with an intrinsically high mitochondrial activity, and several studies indicate that distinct mitochondrial respiratory functions, such as complex I activity, decrease with aging in liver [3], muscle [4] and brain [5]. In mitochondria, electrons are transferred from cytosolic redox reactions to molecular oxygen and this involves the respiratory chain consisting of complexes I–IV. Age-dependent decrease in mitochondrial respiration affects mostly the activity of complexes I, III and IV of the respiratory chain, whereas complex II remains largely unaffected (see [1] for a review). *In situ* staining for cytochrome *c* oxidase (complex IV) has been used to demonstrate the age-associated decrease in mitochondrial function *in vivo* [6]. Using this technology, it was shown that in aged postmitotic tissue, such as muscles or neurons, individual cells with a defect in cytochrome *c* oxidase are detected *in situ* [7], suggesting that some cells lack any functional mitochondria in aged postmitotic tissue.

Age-associated functional impairment is not restricted to postmitotic tissues with high mitochondrial activity, but also occurs in other tissue, such as the skin, where mitochondrial activity is much lower and cells retain at least a part of their proliferative capacity in the adult organism. It is known that proliferating cells, in contrast with postmitotic cells in muscles or brain, produce a large part of their energy from glycolysis instead of mitochondrial ATP production, and it was hypothesized that down-regulation of mitochondrial activity protects such cells from oxidative stress [8]. Based on these findings, one can assume that the role of mitochondria in cellular aging may be quite distinct in different organs; however, little is known about the role of mitochondrial function (and dysfunction) in skin aging.

To explain the decrease in mitochondrial function, a vicious cycle has been described in which deficient mitochondria produce oxygen radicals, which then induce additional damage to the mitochondria, giving rise to even more ROS (reactive oxygen species) ([9]; see [1] for a review). A general model on aging was derived from these findings and it predicts that mitochondrial proteins and mitochondrial DNA are the primary targets of age-associated oxidative damage ([10]; see [11,12] for recent reviews). In an alternative model, the accumulation of damaged mitochondrial DNA could also be due to clonal expansion of individual mutations in mitochondrial genomes, rather than due to a cascade of independent mutations that accumulate over time [6,7]. Taken together, the results available suggest that an age-related decrease in mitochondrial function occurs in postmitotic tissues with intrinsically high mitochondrial activity, and probably contributes to their age-related functional degeneration, although molecular mechanisms remain elusive.

Conventionally, aging processes in humans are studied in cellular models for *in vitro* aging, as pioneered for human dermal fibroblasts by Hayflick and co-workers (see [13] for a review).

Abbreviations used: CS, citrate synthase; FCCP, carbonyl cyanide *p*-trifluoromethoxyphenylhydrazone; LDH, lactate dehydrogenase; PDL, population doubling; ROS, reactive oxygen species; UCP, uncoupling protein.

[1] These authors have contributed equally to this work.

[2] To whom correspondence should be addressed (e-mail erich.gnaiger@uibk.ac.at).

The fibroblast model of replicative senescence has provided fundamental insights into the biology of human aging, such as the role of telomere shortening (see [14] for a review), and continues to reveal key properties of senescent cells that probably occur in aged tissues *in vivo* as well (see [15] for a review). To rule out potentially confounding effects due to cell-cycle effects, it is necessary to compare senescent cells with young cells that are growth-arrested. In a previous study, we analysed the energy metabolism of senescent human fibroblasts *in vitro*, and found that with increasing cellular age, intracellular pools of ATP and other nucleotide triphosphates are depleted and NTP levels are severely decreased [16]. Although part of this energy depletion may be due to the decreased glycolytic capacity in senescent cells [16], it may also reflect decreased energy output from oxidative phosphorylation. These observations raise the possibility that a decrease in mitochondrial function may contribute to replicative senescence. To address this question, we applied high-resolution respirometry to non-permeabilized cells, and adopted a method to determine mitochondrial membrane potential *in situ*, using the fluorescent dye JC-1 in permeabilized cells. With these techniques, we show that, although there is no decrease in respiratory capacity in the mitochondria of senescent fibroblasts, respiratory uncoupling occurs in a subset of the senescent cells. This is not linked to senescence-associated growth arrest, since cell-cycle arrest of young cells, induced by contact inhibition, does not induce respiratory uncoupling. Partial uncoupling might be caused by the enhanced oxidative stress, which was detected in senescent fibroblasts by staining with dihydrorhodamine 123. Taken together, these results suggest that increased oxidative stress is associated with partial uncoupling of oxidative phosphorylation in senescent fibroblasts.

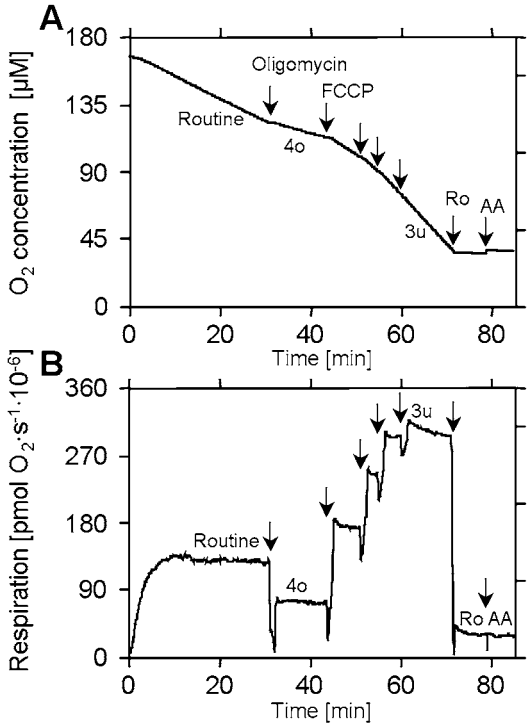

Figure 1 Representative traces of oxygen concentration and respiration of a standard respirometry experiment

(**A**) Trace of oxygen concentration during the experimental titration regime described below. (**B**) Respiration, calculated as the negative timed derivative (slope) of oxygen concentration, in the closed (2 ml) respirometer chamber, in senescent human primary fibroblasts (0.2×10^6 cells/ml). Arrows show steps in the titration regime, inducing the following respiratory states: Routine, routine state in cell-culture medium; Oligomycin and 4o, inhibition of ATP synthase by 1 μg/ml oligomycin to induce the ADP-independent state 4o; FCCP and 3u, maximal stimulation by uncoupling of oxidative phosphorylation in four subsequent titrations of FCCP (2.5–4 μM final concentration), inducing the ADP-independent state 3u; Ro and AA, inhibition by 0.5 μM rotenone and 5 μM antimycin A. Respiration was measured at 37 °C and corrected for instrumental background oxygen flux.

MATERIALS AND METHODS

Cell culture

Normal diploid fibroblasts were isolated from human foreskin [17] and cultured in Dulbecco's modified Eagle's medium (Gibco Life Technologies, Vienna, Austria), supplemented with penicillin/streptomycin solution (Gibco Life Technologies) and 10 % (v/v) foetal calf serum (Gibco Life Technologies). The culture medium contained substrates for cellular energy metabolism, such as glucose (5 mM), pyruvate (1 mM) and L-glutamine (4 mM). The cells were subcultured in an atmosphere of 5 % CO_2 in air at 37 °C by passaging them at a ratio of 1:5 at regular intervals. For passages in aged cells, the splitting ratio was progressively decreased to 1:3 and 1:2. PDL (population doubling) was estimated using the equation $PDL = (\ln F - \ln I)/\ln 2$, where F is the number of cells at the end of one passage and I the number of cells that were seeded at the beginning of one passage. After approx. 55 PDL, the cells reached growth arrest. The senescent status was verified by *in situ* staining for senescence-associated β-galactosidase as described in [18]. G_0 arrest of young fibroblasts was achieved by contact inhibition, growing cells to 100 % confluence and subsequent feeding for another 5 days. In the present study, young proliferating and density-arrested fibroblasts were used at passage 13 (corresponding to 20 PDL), whereas senescent fibroblasts were used at passage 28 (corresponding to 50 PDL).

For respirometric experiments, cells were cultured in 75 cm^2 flasks. The cells were harvested enzymically by a solution of 0.25 % trypsin/1 mM EDTA. Trypsin activity was stopped by adding a culture medium containing 10 % foetal calf serum. Cells were spun at 155 ***g*** for 10 min and finally resuspended in 3 ml of Dulbecco's modified Eagle's medium without Phenol Red (Sigma, Vienna, Austria). Omission of Phenol Red improved the visibility for observation of the cell suspension in the oxygraph chamber.

High-resolution respirometry

Respiration was measured at 37 °C by high-resolution respirometry using the Oroboros® oxygraph with chamber volumes set at 2 ml. DatLab software (Oroboros Instruments, Innsbruck, Austria) was used for data acquisition (1 or 2 s time intervals) and analysis, which includes online calculation of the time derivative of oxygen concentration and correction for instrumental background oxygen flux [19]. The experimental regime started with routine respiration, which is defined as respiration in cell-culture medium without additional substrates or effectors. After observing steady-state respiratory flux in the time interval between 15 and 30 min after closing the chamber, the ATP synthase was inhibited with oligomycin (1 μg/ml), followed by uncoupling of oxidative phosphorylation by stepwise titration of FCCP (carbonyl cyanide *p*-trifluoromethoxyphenylhydrazone) up to optimum concentrations in the range of 2.5–4 μM (Figure 1). Finally, respiration was inhibited by sequential addition of rotenone at 0.5 μM (to test for the effect of inhibiting complex I activity) and antimycin A at 2.5 μM (inhibiting complex III). This titration method was completed within 90 min. Intermittent

re-aerations were performed if necessary to avoid limitation of oxygen for respiration [20].

Cell count, spectrophotometric enzyme and protein assays

For the determination of cell number (CASY 1 Cell Counter and Analyser System, Schärfe System, Reutlingen, Germany), 120 μl of the sample was taken from the cell suspension stirred in the oxygraph chamber. In addition, two portions of 300 μl of the sample were taken for duplicate CS (citrate synthase) and LDH (lactate dehydrogenase) assays respectively before the chamber was closed for recording respiration. Samples were frozen in liquid nitrogen and stored at -80 °C. The activity of CS was measured spectrophotometrically at 412 nm and 30 °C. Cell lysate (100 μl) was added to 900 μl of medium containing 0.1 mM 5,5-dithio-bis-(2-nitrobenzoic) acid (DTNB), 0.5 mM oxaloacetate, 50 μM EDTA, 0.31 mM acetyl CoA, 5 mM triethanolamine hydrochloride and 0.1 M Tris/HCl (pH 8.1) [21]. LDH activity was measured at 340 nm and 30 °C [22] using 100 μl of cell lysate in a 0.1 M Tris/HCl buffer (Merck, West-Point, PA, U.S.A.) with 0.25 % Triton X-100 (Serva, Vienna, Austria) at pH 7.1, with 10 mM pyruvate and 0.3 mM NADH (Fluka, St. Louis, MO, U.S.A.).

For protein measurements, the cell suspension was taken from the oxygraph chamber after completion of respirometric runs, washed three times, resuspended in PBS (Gibco Life Technologies) and frozen in liquid nitrogen. The protein content was measured by the Bradford assay (Bio-Rad, Hercules, CA, U.S.A.) using γ-globulin as a standard in the linear range 1.45–0.09 mg/ml.

Confocal laser scanning microscopy

Cells were grown overnight on 60 mm diameter culture dishes and incubated for 30 min with MitoTracker® RedCMXRos (Molecular Probes) at a final concentration of 25 nM in culture medium. After incubation, the cells were washed twice with PBS and staining was analysed by confocal laser scanning microscopy, using a Bio-Rad μRadiance device, combined with a Zeiss Axiophot microscope.

For the determination of mitochondrial membrane potential, we used the potentiometric dye JC-1. It is known from the literature that the plasma-membrane potential influences the capability of cells to take up JC-1, as reported by Bernardi et al. [23]; hence, we used a method in which the influence of the plasma-membrane potential on the uptake of the dye was abolished by permeabilization of the plasma membrane [24] with an optimum concentration of digitonin (20 μg/ml; Sigma, catalogue no. D-1407) in the mitochondrial medium MiR05, which was determined as described previously [25]. Permeabilization efficiency was controlled by propidium iodide staining. The dye was applied to the cells in MiR05 at a final concentration of 3 μg/ml and propidium iodide uptake was monitored by fluorescence microscopy. JC-1 was tested at concentrations of 0.5 and 1.0 μg/ml with these permeabilized cells, showing only minor differences. For JC-1 staining, cells were grown overnight on 60 mm dishes, washed with PBS and incubated in MiR05, to which 20 μg/ml digitonin, 10 mM succinate (Merck, Darmstadt, Germany), 0.5 μM rotenone and 0.5 μg/ml JC-1 (Molecular Probes, Leiden, The Netherlands) were added. After 15 min incubation, cells were washed with MiR05, supplemented with 10 mM succinate, and analysed by confocal laser scanning microscopy. MiR05 consisted of 110 mM sucrose, 60 mM potassium lactobionate (Fluka Chemie, Vienna, Austria), 0.5 mM EGTA, 1 g/l BSA essentially fat-free, 3 mM $MgCl_2$, 20 mM taurine (Merck, Germany), 10 mM KH_2PO_4 (Merck, Germany), 20 mM Hepes adjusted to pH 7.1 with KOH at 37 °C [26]. A standardized mitochondrial resting state was obtained by electron supply from the complex II substrate, succinate, in the presence of the complex I inhibitor, rotenone. Under these conditions, maximum mitochondrial membrane potential is maintained by state 2 respiration. After confocal laser scanning microscopy, the same cells were uncoupled and inhibited by a high concentration (20 μM) of FCCP (see [27]) and another image was obtained to define the reference point of minimum mitochondrial membrane potential.

Preparation of cell extracts and Western-blot analysis

To prepare whole cell extracts, cells were either trypsinized from culture flasks and washed with PBS (to generate lysates of equal cell quantities), or washed twice with ice-cold PBS and scraped from the culture dish with a rubber policeman (to generate lysates of equal protein concentrations). Cells were lysed for 30 min on ice in a buffer containing 50 mM Tris/HCl (pH 7.5), 300 mM NaCl, 1 % Nonidet P40, 0.1 % SDS, 0.5 % sodium deoxycholate, 0.2 mM PMSF, 1 mM NaF, 10 μg/ml aprotinin, 10 μg/ml leupeptin and 10 mM β-glycerophosphate. The lysates were centrifuged at 20000 ***g*** for 15 min at 4 °C, and the supernatants were separated on SDS/polyacrylamide gels. Protein concentrations were determined by using the DC Protein Assay kit (Bio-Rad). The amounts of loaded extract corresponded either to equal cell quantities or equal protein concentrations, depending on the experimental setting. After electrophoresis, the proteins were transferred on to nitrocellulose membranes by wet electroblotting in a buffer containing 25 mM Tris/HCl, 190 mM glycine, 0.5 % SDS and 10 % (v/v) methanol. Transfer was controlled by staining the membrane with Ponceau S. Membranes were blocked by incubation in 5 % (w/v) non-fat dried milk in TBS-T (Tris-buffered saline + 0.1 % Tween 20) for 1 h at room temperature (22 °C). Incubation with the primary antibody was performed for 60 min at room temperature or overnight at 4 °C. Membranes were washed twice with TBS-T and incubated with the secondary antibody for 30 min. After four washes with TBS-T and one wash with TBS, immunoreactive proteins were detected using an enhanced chemiluminescence system (Amersham Biosciences). The following antibodies were used for Western-blot analysis: polyclonal rabbit anti-cytochrome *c* (sc-7159; Santa Cruz Biotechnology, Heidelberg, Germany), polyclonal goat anti-AIF (where AIF stands for apoptosis-inducing factor; sc-9416; Santa Cruz Biotechnology), monoclonal mouse anti-CS (MAB3087; Chemicon, Temecula, CA, U.S.A.), polyclonal goat anti-UCP-2 (where UCP stands for uncoupling protein) (sc-6525; Santa Cruz Biotechnology), monoclonal mouse anti-cyclin D1 (DCS-11; NeoMarkers, Fremont, CA, U.S.A.), monoclonal mouse anti β-actin (clone AC-15; Sigma); all secondary antibodies were obtained from Promega, except for the anti-goat antibody (Dako, Glostrup, Denmark).

Chemicals

All the chemicals were purchased from Sigma unless indicated otherwise.

Statistical analyses

Results are expressed as means $\pm$ S.D. Statistical analyses were performed using Mann–Whitney U test, and $P < 0.05$ was taken as the level of significance.

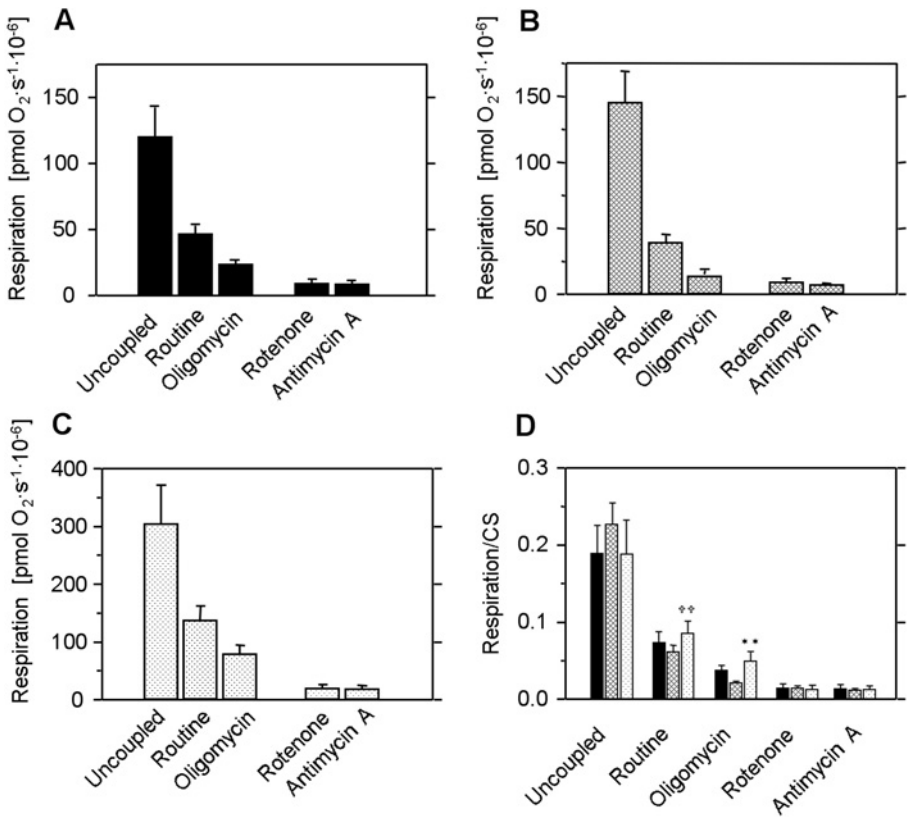

Figure 2 Respiration (pmol of $O_2 \cdot s^{-1} \cdot 10^{-6}$ cells) of human primary foreskin fibroblasts in various states of mitochondrial respiratory control

(**A**) Respiration of young (20 PDL) proliferating fibroblasts. Bars represent the means ± S.D. for 12 parallel experiments. (**B**) Respiration of young (20 PDL) density-arrested fibroblasts. Bars represent the means ± S.D. for five parallel experiments. (**C**) Respiration of senescent (50 PDL) fibroblasts. Bars represent the means ± S.D. for 12 parallel experiments. (**D**) Respiratory parameters normalized by CS activity (pmol $\cdot s^{-1} \cdot 10^{-6}$ cells). Respiratory flux of proliferating fibroblasts is compared with results from arrested and senescent fibroblasts respectively. Values were normalized by CS activity that was determined in parallel. $^{**}P < 0.01$, with respect to young proliferating and arrested controls; $\dagger\dagger P < 0.01$, with respect to density-arrested young control cells.

RESULTS

Respiratory capacity and mitochondrial content

To investigate age-related alterations of mitochondria in diploid human fibroblasts, mitochondrial respiratory function in young and senescent fibroblasts was analysed in a standardized experimental regime (Figure 1). Since senescent fibroblasts are irreversibly arrested in the G_1 phase of the cell cycle [28], young cell-cycle-arrested fibroblasts were included as a second control. Respiratory capacity per cell, measured after uncoupling with FCCP (Figure 1), was increased in senescent cells by approx. 2-fold compared with both the control groups (Figure 2). Uncoupled respiration was not significantly different in the control groups, amounting to 120 ± 23 pmol of $O_2 \cdot s^{-1} \cdot 10^{-6}$ cells ($n = 12$) in young proliferating fibroblasts (Figure 2A) and 145 ± 23 pmol of $O_2 \cdot s^{-1} \cdot 10^{-6}$ cells ($n = 5$) in young density-arrested cells (Figure 2B). Similar values for uncoupled oxygen consumption have been obtained previously with other cell types, e.g. endothelial cells [27] or lymphocytes [26]. Respiration was inhibited by rotenone and antimycin A to an equal extent in senescent cells and both of the young control groups (Figures 2A–2C). Relative to uncoupled respiration, antimycin A-inhibited rates amounted to $7 \pm 3\%$ in young proliferating cells, $5 \pm 0.4\%$ in young density-arrested cells and $7 \pm 3\%$ in senescent cells. This indicates the predominant contribution ($> 90\%$) of mitochondria to the total cellular oxygen consumption. Respiration per cell was increased in senescent fibroblasts in both coupled and uncoupled states when compared with young cells (Figures 2A–2C).

Table 1 Analysis of CS and LDH activities

Enzyme velocities V_{CS} and V_{LDH} are expressed in terms of $\mu mol \cdot min^{-1} \cdot 10^{-6}$ cells. PDL 20 proliferating, young proliferating fibroblasts ($n = 12$); PDL 20 arrested, young density-arrested fibroblasts ($n = 6$); PDL 50, senescent fibroblasts ($n = 12$).

Fibroblasts	V_{CS}	V_{LDH}	LDH/CS
PDL 20 proliferating	0.039 ± 0.011	221 ± 38	5.840 ± 1.140
PDL 20 arrested	0.042 ± 0.010	189 ± 44	4.530 ± 240
PDL 50 senescent	0.098 ± 0.012*†	897 ± 154*†	9.280 ± 1.770*†

* $P < 0.01$, with respect to young proliferating cells.
† $P < 0.01$, for density-arrested controls.

To relate the increased respiration per cell observed in senescent fibroblasts to mitochondrial content, we measured the activity of the mitochondrial matrix marker enzyme CS and normalized respiratory parameters to CS activity. CS activity was increased in senescent fibroblasts to a similar extent as observed for respiration (Table 1). Therefore, based on uncoupled respiration as normalized to CS (Figure 2D), no significant differences in the capacity of the respiratory chain were observed between senescent cells and both of the young control groups.

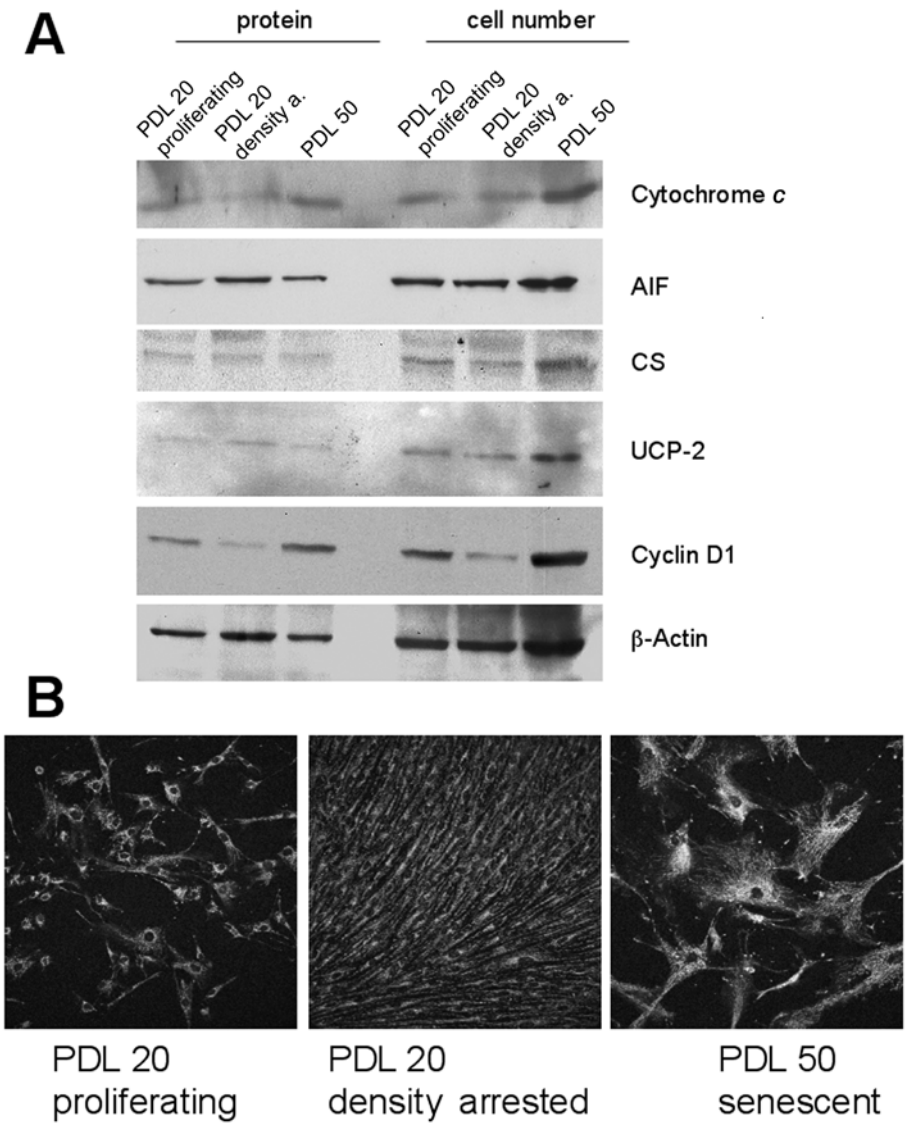

Figure 3 Analysis of mitochondrial content in human primary fibroblasts

(**A**) Western-blot analysis of mitochondrial proteins. Expression of the cell-cycle regulator protein, cyclin D1, was used as a reference. Results are expressed either in terms of equal protein concentrations or equal cell numbers. Expression levels were normalized by β-actin. (**B**) Representative confocal images of mitochondrial staining with MitoTracker® RedCMXRos. density a., density-arrested.

Western-blot analysis revealed an increase in the amount of CS in senescent cells, when equal cell numbers were analysed (Figure 3A), corresponding to the change in CS activity. However, the amount of CS was not increased to a detectable level when Western blots were normalized for equal protein loading (Figure 3A). During cellular aging, both the protein and enzymic activities of CS increased by approx. 2-fold, in line with the increased cell volume, total protein content and cellular respiration that occur with replicative age (Table 2). The levels of AIF [29] and cytochrome *c*, both located in the intermembrane space, were not significantly altered with cellular aging when equal amounts of cellular protein were loaded for Western blotting. Similarly, the abundance of UCP-2 [30], spanning the inner mitochondrial membrane, was unchanged when loading equal protein concentrations, whereas normalization to cell number revealed the approx. 2-fold increase in signal that was observed for all mitochondrial components (Figure 3A). These results indicate that the mitochondrial content increased in senescent cells as a function of cell size, whereas mitochondrial density remained constant, supporting the results obtained from enzymic assays.

Table 2 Cell volume and protein content of young and senescent fibroblasts

Values are expressed as means ± S.D. for six parallel experiments, except for the cell volume of proliferating and senescent cells (12 experiments).

Fibroblasts	Cell volume (pl/cell)	Protein (mg/10^6 cells)
PDL 20 proliferating (12 experiments)	2.58 ± 0.30	3.56 ± 0.51
PDL 20 arrested (six experiments)	2.15 ± 0.22	3.93 ± 0.69
PDL 50 senescent (12 experiments)	9.91 ± 0.93*†	7.40 ± 0.69*†

* $P < 0.01$, with respect to young proliferating cells.
† $P < 0.01$, for density-arrested controls.

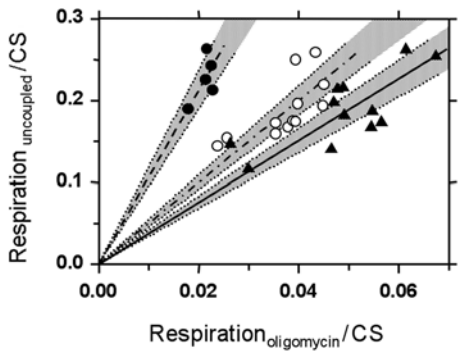

Figure 4 Coupling state of oxidative phosphorylation in human fibroblasts

The relation between uncoupled and oligomycin-inhibited respirations is shown; respiratory parameters were normalized by CS activity; ○, proliferating fibroblasts ($n = 12$); ●, density-arrested fibroblasts ($n = 5$); ▲, senescent fibroblasts ($n = 12$); thick solid lines represent linear regressions. Confidence intervals are shaded for the regressions forced through the origin.

This conclusion was further confirmed by fluorescence staining of mitochondria with MitoTracker® Red (Figure 3B) and by transmission electron microscopy (E. Hutter, W. Salvenmoser, R. Rieger, P. Jansen-Durr, unpublished work). Taken together, our results demonstrate that the increased mitochondrial respiration in senescent fibroblasts was due to an increase in mitochondrial content. As described previously [31], cyclin D1 was down-regulated in density-arrested human fibroblasts, whereas it was up-regulated in senescent fibroblasts (Figure 3A).

LDH activity and LDH/CS ratio

Although mitochondrial density was largely maintained in old fibroblasts, it is known that in senescent cells a reprogramming of the carbohydrate metabolism occurs. This results in imbalances of the glycolytic apparatus, e.g. a strong up-regulation of LDH activity [16]. In the present study, this was confirmed in terms of an increased LDH/CS ratio in senescent cells compared with young cells (Table 1). Growth arrest was ruled out as a trigger for this shift in glycolytic/oxidative enzyme ratio, since the LDH/CS ratio was even lower in density-arrested young cells when compared with young proliferating cells (Table 1).

Respiratory control and coupling

To study further age-associated changes in mitochondrial function, mitochondrial coupling states were analysed. Respiratory control ratios were determined from titrations with the ATP synthase inhibitor oligomycin and the uncoupler FCCP. These ratios yield important information on the control of electron flux through the respiratory chain by the ATP synthase. Importantly, oligomycin-inhibited respiration, as normalized to CS, was significantly increased in senescent cells when compared with controls (Figure 2D). Uncoupled respiration, as normalized to CS, increased linearly as a function of oligomycin-inhibited respiratory rates, as normalized to CS, but with non-identical slopes in the different experimental groups (Figure 4). These slopes reflect the ratio of uncoupled respiration to oligomycin-inhibited respiration (respiratory control ratio, referred to as $j_{3u/4o}$), which was significantly decreased in senescent cells (Table 3). In conjunction with the constant respiratory capacity (per CS), this indicates partial uncoupling in senescent fibroblasts. The ratio of uncoupled respiration to routine respiration (uncoupling control ratio, referred to as $j_{3u/R}$) was also significantly decreased in senescent cells. The $j_{3u/R}$ in proliferating fibroblasts was 2.58 ± 0.21 ($n = 12$); in young density-arrested fibroblasts, it increased to 3.72 ± 0.15 ($n = 5$), whereas in senescent cells the $j_{3u/R}$ decreased to 2.21 ± 0.23 ($n = 12$).

Table 3 Respiratory control ratio ($j_{3u/4o}$) and index of respiration coupled with ATP production ($j_{(R-4o)/3u}$)

R, routine respiration; 4o, oligomycin-inhibited respiration; 3u, uncoupled respiration. To calculate the proportion of phosphorylation-related respiration ($j_{(R-4o)/3u}$), we normalized the difference between routine and oligomycin-inhibited respirations ($R - 4o$) with total mitochondrial capacity (3u).

Fibroblasts	$j_{3u/4o}$	$j_{(R-4o)/3u}$
PDL 20 proliferating (12 experiments)	5.1 ± 0.8	0.19 ± 0.01
PDL 20 arrested (five experiments)	10.7 ± 1.0	0.17 ± 0.02
PDL 50 senescent (12 experiments)	3.9 ± 0.7*†	0.19 ± 0.05

* $P < 0.01$, with respect to young proliferating cells.
† $P < 0.01$, for density-arrested controls.

Partial uncoupling may lead to a diminished oxidative ATP production or to a compensatory increase in electron transport. To distinguish between these alternatives, we subtracted oligomycin-inhibited respiration from routine respiration ($R - 4o$), which allowed us to determine the part of respiratory activity coupled with ATP production. Despite substantial differences in the $j_{3u/4o}$, ranging from 4 to 11 in the different experimental groups, a fixed proportion of respiratory capacity was maintained for coupled oxidative phosphorylation in all the experimental groups (Table 3). This finding indicates that the senescent cells fully compensate for increased proton leakage by enhanced electron transport activity in the routine state.

Senescence-associated changes in mitochondrial membrane potential

The decreased $j_{3u/4o}$ observed in senescent cells may be due to partial uncoupling of the respiratory chain in all cells or, alternatively, it could result from stronger respiratory uncoupling in a subpopulation of cells, whereas respiratory function would be well preserved in a majority of the cell population. To discriminate between these possibilities, we analysed heterogeneity of mitochondrial membrane potential at the single cell level. Cells were permeabilized, stained by JC-1, a potentiometric dye that is suitable for detecting changes in mitochondrial membrane potential (see [32] for a review), and imaged by confocal microscopy. As shown by propidium iodide staining, 20 μg/ml digitonin fully permeabilized the plasma membrane without affecting mitochondrial integrity [25], whereas no propidium iodide uptake was observed in cells without digitonin treatment (Figure 5A). Figure 5(B) shows representative confocal images of cells stained with JC-1. The shift from red to green after the addition of FCCP reflects the specific response of JC-1 to the dissipation of mitochondrial membrane potential by uncoupling. Mitochondria of young proliferating and density-arrested controls exhibited bright red fluorescence in the absence of FCCP, corresponding to highly energized mitochondria in the coupled state. Most of the senescent cells exhibited predominantly bright red fluorescence. A subpopulation of senescent fibroblasts, however, displayed patches of green fluorescence, which was absent from other senescent cells and in all control cells. This distinct green fluorescence in old cells reflects a subpopulation

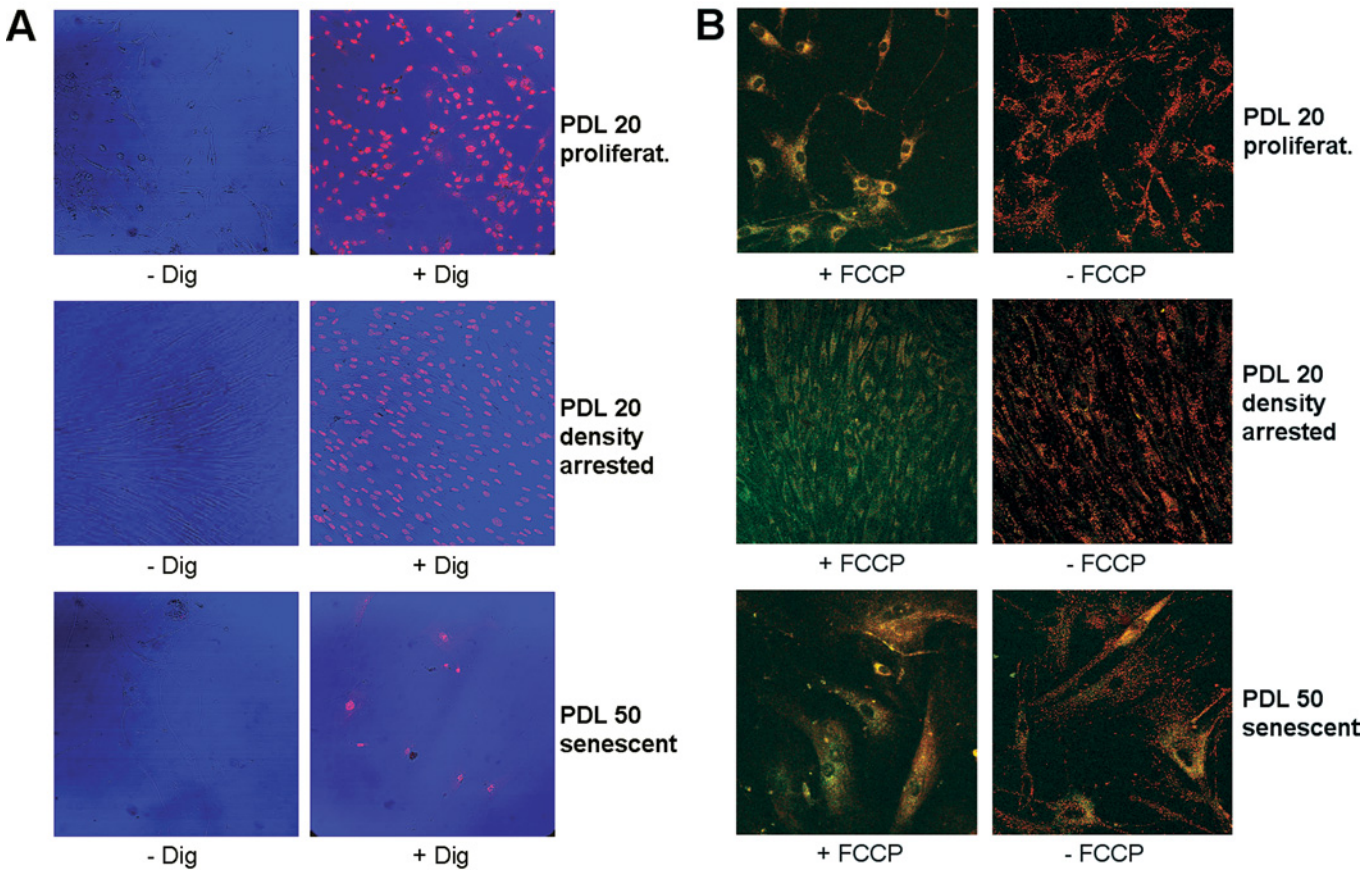

Figure 5 Analysis of mitochondrial membrane potential in young and old fibroblasts

Cells were permeabilized with 20 μg/ml digitonin. Young fibroblasts [20 PDL, proliferating (proliferat.) or density-arrested]; senescent fibroblasts (50 PDL). (**A**) Nuclear staining with propidium iodide, used as control for full permeabilization of the plasma membrane; − Dig, unpermeabilized cells in MiR05; + Dig, cells permeabilized with digitonin in MiR05. (**B**) Mitochondrial staining of permeabilized cells with JC-1 (0.5 μg/ml final concentration). Where indicated, FCCP was added to the cells at a final concentration of 20 μM.

of mitochondria with a lower membrane potential, supporting the conclusions drawn from the respirometric measurements on a partial decrease in the coupling state. Importantly, de-energized mitochondria did not appear before the cells were > 95 % positive for β-galactosidase (results not shown).

Taken together, these results demonstrate that mitochondrial respiratory capacity was not impaired in senescent fibroblasts. Partial uncoupling of oxidative phosphorylation, however, occurred in a subpopulation of senescent cells, which was compensated by an activation of routine respiration relative to respiratory capacity.

DISCUSSION

Study of mitochondrial respiratory parameters provides an important tool to understand mitochondrial physiology and the potential role of mitochondrial pathologies in cellular aging processes. To answer the question whether mitochondrial defects contribute to the phenotype of cellular senescence, we analysed the specific mitochondrial respiratory functions of young and senescent fibroblasts. To distinguish between age-related and cell-cycle arrest-related effects, we used young cell-cycle-arrested fibroblasts as an additional control group for this model of senescence. Importantly, significant differences in mitochondrial respiratory control were found between proliferating and non-proliferating young fibroblasts, which underscores this consideration of the appropriate control group. Respirometry was performed in cell-culture medium, with all external substrates necessary for growth and energy metabolism, without permeabilization of cells. In this respect, our studies allow us to integrate regulatory events by which cytoplasmic and nuclear factors influence mitochondrial function, and hence differ from respiratory analyses on isolated mitochondria.

Our results indicate partial uncoupling of mitochondrial respiration in senescent fibroblasts with respect to both the control groups, suggesting that a functional deterioration of mitochondria occurs with cellular aging. In the following sections, we will discuss the consequences of our findings with respect to cellular energy production and the maintenance of mitochondrial membrane potential and consider possible effects on ROS production and the cellular redox state.

Partial uncoupling and oxidative phosphorylation in young and senescent cells

The ratio of uncoupled respiration to routine respiration (uncoupling control ratio $j_{3u/R}$) in proliferating fibroblasts was 2.6, similar to the $j_{3u/R}$ in other cell types (2.5–3.5 in human umbilical-vein endothelial cells [27]; 2.5–2.7 in transformed endothelial cells [33,34]; and 2.5 in leukaemia cells [26]). This indicates a high respiratory reserve capacity, since uncoupled respiration is 2.5–3 times higher compared with the respiratory activity observed under physiological conditions in these cultured cells.

In density-arrested young fibroblasts, $j_{3u/R}$ was increased to 3.7, which was significantly higher than the $j_{3u/R}$ obtained in young proliferating cells. Since the respiratory capacity remained unchanged, this may be caused by down-regulation of the proton leakage (or slip) in non-growing cells. Alternatively, a decreased oxidative ATP demand in non-growing cells would result in a higher $j_{3u/R}$, reflecting a metabolic state where routine respiration utilizes an even lower proportion of maximum capacity (see [35] for a review). A distinction between down-regulation of mitochondrial activity by either tighter coupling or by reduced ATP demand is possible on the basis of the respiratory control ratio (the ratio of uncoupled respiration to state 4o respiration $j_{3u/4o}$). In the oligomycin-inhibited state 4o, proton backflow through the ATP synthase is inhibited, the mitochondrial membrane potential is increased by proton pumping and steady-state respiration compensates for proton leakage. In growing fibroblasts, $j_{3u/4o}$ was 5.1 and increased to 10.7 in non-growing young cells, clearly indicating a tighter coupling in arrested cells. In comparison, the $j_{3u/4o}$ of senescent (non-growing) cells was as low as 3.9. Since cell-cycle arrest exerted a significant effect on respiratory coupling in young cells, the non-proliferating state represents the relevant control group for evaluation of aging-related respiratory changes. The largest difference in coupling states was observed between this control group and senescent cells, thus excluding cell-cycle effects as a cause for partial uncoupling in aged fibroblasts. In addition, this decrease in the respiratory control ratio was significant with respect to the proliferating control group (Table 3). Others have reported that mitochondrial respiratory function does not change with the passaging of human diploid fibroblasts [36]. In those studies, however, no systematic analysis of the coupling state was performed. Moreover, truly senescent fibroblasts (i.e. cells at the end of their replicative lifespan) were not analysed in [36].

To address the question whether partial uncoupling diminished oxidative phosphorylation or was compensated by respiratory control mechanisms, we analysed phosphorylation-related respiration and found that a constant rate of oxidative phosphorylation is maintained, as described in Table 3. In all the experimental groups, approx. 18 % of respiratory capacity was under adenylate control under routine respiratory conditions, thus indicating compensation for partial uncoupling by increased routine respiration and excluding increased mitochondrial ATP production in senescent versus young fibroblasts. Despite the fact that senescent cells contain high AMP levels [16,37], oxidative phosphorylation was not increased in these cells. Since the uncoupler-stimulated respiratory capacity (per CS) was comparable in young and senescent cells, substrate supply and mitochondrial electron transport are excluded as potentially limiting factors. We previously found an impairment of aerobic glycolysis in senescent cells, which contributes to the observed decrease in the ATP/AMP ratio [16]. In this respect, it is surprising that the increased levels of AMP do not induce respiratory activity, despite the excess capacity of the electron-transport system. Others have observed age-associated oxidative damage of adenine nucleotide translocase [38]. In line with this enzyme-specific ROS-induced defect, our experiments do not exclude the possibility that AMP-dependent activation of respiration is limited by the phosphorylation system (adenylate and phosphate transport systems, ATP synthase) in senescent cells. In this context, up-regulation of the adenylate kinase in senescent fibroblasts [16] may be interpreted as an adaptive mechanism triggered by a defect in the phosphorylation system.

Mitochondrial uncoupling can arise from oxidative damage of the mitochondrial membrane as induced by increased ROS concentrations [34]. In fact, both partial uncoupling (see above) and enhanced oxidative stress were observed in senescent human fibroblasts: senescent cells display strongly enhanced staining with dihydrorhodamine 123 (E. Hutter, H. Unterluggauer, P. Stockl and P. Jansen-Durr, unpublished work), which is taken as an indication of increased ROS levels, together with a higher extent of oxidatively damaged proteins, detected as carbonylated proteins (E. Hutter, H. Unterluggauer, P. Stockl and P. Jansen-Durr, unpublished work). In addition to activation of the permeability transition pore (see [39]), as shown in mitochondria from various tissues of aging mice [40,41], unspecific leakage of protons could occur in mitochondria of senescent fibroblasts due to increased ROS levels. In this respect, it is interesting to note that gross ultrastructural defects in mitochondria were not observed in senescent cells [42,43], which is in agreement with our own electron microscopic studies (E. Hutter, W. Salvenmoser, R. Rieger and P. Jansen-Durr, unpublished work). Although this observation does not exclude that functional damage to mitochondrial membranes occurs in senescent cells, other mechanisms may also contribute to respiratory uncoupling.

UCPs shortcut electron flux through mitochondrial membranes; apart from the tissue-specific members of the UCP family, namely UCP-1 and -3, a third family member, UCP-2, is more broadly expressed (see [44] for a review). We show in the present study that diploid human fibroblasts also expressed UCP-2 and the relative abundance of UCP-2 was not increased in senescent cells (Figure 3A). UCP-2 is known to be activated by ROS [45] and the increased abundance of ROS that is detected in senescent cells could contribute to the decreased coupling state observed in senescent fibroblasts. However, more work will be required to assess the functional status of UCP-2 in senescent cells.

Senescence-associated changes in mitochondrial membrane potential

Mitochondrial membrane potential is frequently studied with the use of potentiometric fluorescent dyes, although this method has some intrinsic problems if used inappropriately [23]. In the present study, we developed a method for JC-1 staining in permeabilized cells to rule out influences of the plasma membrane on dye uptake (cf. [24] for a similar staining method). This approach revealed a subpopulation of senescent cells with de-energized mitochondria, in agreement with the partial uncoupling revealed by high-resolution respirometry. The appearance of cells with de-energized mitochondria was not a sudden event, but such cells accumulated steadily towards the end of the replicative lifespan. This suggests that mitochondria with impaired respiratory function accumulate in the postmitotic state. This is in contrast with the work of Goldstein and Korczack [46], who reported a general decrease in mitochondrial membrane potential in pre-senescent human fibroblasts. However, Goldstein and Korczack [46] deduced the mitochondrial membrane potential from experiments applying the fluorescent dye rhodamine 123, which may not be a reliable probe to assess mitochondrial membrane potential [47]. In other studies using rhodamine 123, it was concluded that senescent fibroblasts maintain a higher mitochondrial transmembrane potential compared with young cells [48,49], clearly contradicting the results reported here.

Conclusion

Substantial evidence in the literature suggests that organismic aging is correlated with increasing damage to mitochondria [12] and decay of mitochondrial function has been invoked as a major determinant of aging [11]. The mitochondrial theory of aging

predicts that, over the lifespan of an organism, increasing damage (predominantly oxidative damage) occurs in the mitochondrial genome and/or mitochondrial proteins, and ROS (predominantly superoxide) are produced in the mitochondria (either chronically during normal mitochondrial function or increased production as a result of mitochondrial damage). Although this is a very attractive hypothesis, the theory has been difficult to prove due to the lack of appropriate experimental systems. In particular, the molecular mechanisms underlying ROS production and the essential cellular targets of ROS have remained elusive. Moreover, the molecular nature of the damage underlying mitochondrial dysfunction in aging tissue is unclear at present. The findings reported here suggest the appearance of cells with uncoupled mitochondria as a key property of cellular aging *in vitro*. The differences in the degree of coupling observed between proliferating and growth-arrested young control groups underscore the importance of considering cell-cycle effects. It is noteworthy that most fibroblasts *in vivo* are actually found in non-proliferating states. A very recent study of mitochondrial function in skin fibroblasts derived from donors of different age groups suggests that respiratory uncoupling occurs in a subpopulation of old donors aged >90 years [50], similar to the findings reported here for senescent fibroblasts. Moreover, Greco et al. [50] identified that in that subgroup of very old donors, the decreased respiratory coupling of mitochondria is compensated by an increase in routine respiration, similar to the findings reported here for senescent fibroblasts. These results suggest that at least some of our findings with senescent fibroblasts reflect changes that are observed also during aging *in vivo*; hence, it can be expected that further studies with the experimental approach described here will contribute to a better understanding of the role of mitochondria in skin aging.

This work was supported by the Austrian Science Foundation (FWF project no. 16213-B04), the European Union (CELLAGE project QLK.6-CT-2001-00616) and the Austrian Ministry of Science and Traffic.

REFERENCES

1 van Remmen, H. and Richardson, A. (2001) Oxidative damage to mitochondria and aging. Exp. Gerontol. **36**, 957–968
2 Harman, D. (1956) Aging: a theory based on free radical and radiation chemistry. J. Gerontol. **11**, 298–300
3 Torres-Mendoza, C. E., Albert, A. and de la Cruz Arriaga, M. J. (1999) Molecular study of the rat liver NADH:cytochrome *c* oxidoreductase complex during development and ageing. Mol. Cell. Biochem. **195**, 133–142
4 Feuers, R. J. (1998) The effects of dietary restriction on mitochondrial dysfunction in aging. Ann. N.Y. Acad. Sci. **854**, 192–201
5 Itoh, K., Weis, S., Mehraein, P. and Muller-Hocker, J. (1996) Cytochrome *c* oxidase defects of the human substantia nigra in normal aging. Neurobiol. Aging **17**, 843–848
6 Cottrell, D. A., Blakely, E. L., Johnson, M. A., Borthwick, G. M., Ince, P. I. and Turnbull, D. M. (2001) Mitochondrial DNA mutations in disease and ageing. Novartis Found. Symp. **235**, 234–243
7 Cottrell, D. A., Blakely, E. L., Johnson, M. A., Ince, P. G. and Turnbull, D. M. (2001) Mitochondrial enzyme-deficient hippocampal neurons and choroidal cells in AD. Neurology **57**, 260–264
8 Brand, K. (1997) Aerobic glycolysis by proliferating cells: protection against oxidative stress at the expense of energy yield. J. Bioenerg. Biomembr. **29**, 355–364
9 Sohal, R. S. and Dubey, A. (1994) Mitochondrial oxidative damage, hydrogen peroxide release, and aging. Free Radical Biol. Med. **16**, 621–626
10 Wallace, D. C. (2001) A mitochondrial paradigm for degenerative diseases and ageing. Novartis Found. Symp. **235**, 247–263; discussion 263–266
11 Jacobs, H. T. (2003) The mitochondrial theory of aging: dead or alive? Aging Cell **2**, 11–17
12 Kowald, A. (2001) The mitochondrial theory of aging. Biol. Signals Recept. **10**, 162–175
13 Hayflick, L. (1992) Aging, longevity, and immortality *in vitro*. Exp. Gerontol. **27**, 363–368
14 Shay, J. W. and Wright, W. E. (2001) Telomeres and telomerase: implications for cancer and aging. Radiat. Res. **155**, 188–193
15 Krtolica, A. and Campisi, J. (2003) Integrating epithelial cancer, aging stroma and cellular senescence. Adv. Gerontol. **11**, 109–116
16 Zwerschke, W., Mazurek, S., Stockl, P., Hutter, E., Eigenbrodt, E. and Jansen-Durr, P. (2003) Metabolic analysis of senescent human fibroblasts reveals a role for adenosine monophosphate in cellular senescence. Biochem. J. **376**, 403–411
17 Durst, M., Dzarlieva-Petrusevska, R. T., Boukamp, P., Fusenig, N. E. and Gissmann, L. (1987) Molecular and cytogenetic analysis of immortalized primary human keratinocytes obtained after transfection with human papillomavirus type 16 DNA. Oncogene **1**, 251–256
18 Dimri, G. P., Lee, X., Basile, G., Acosta, M., Scott, G., Roskelley, C., Medrano, E. E., Linskens, M., Rubelj, I., Pereira-Smith, O. et al. (1995) A biomarker that identifies senescent human cells in culture and in aging skin *in vivo*. Proc. Natl. Acad. Sci. U.S.A. **92**, 9363–9367
19 Gnaiger, E. (2001) Bioenergetics at low oxygen: dependence of respiration and phosphorylation on oxygen and adenosine diphosphate supply. Respir. Physiol. **128**, 277–297
20 Hutter, E., Renner, K., Jansen-Durr, P. and Gnaiger, E. (2002) Biphasic oxygen kinetics of cellular respiration and linear oxygen dependence of antimycin A inhibited oxygen consumption. Mol. Biol. Rep. **29**, 83–87
21 Kuznetsov, A. V., Strobl, D., Ruttmann, E., Konigsrainer, A., Margreiter, R. and Gnaiger, E. (2002) Evaluation of mitochondrial respiratory function in small biopsies of liver. Anal. Biochem. **305**, 186–194
22 Bergmeyer, H. U. E. (1974) Methoden der enzymatischen Analyse, vols. I and II, 3rd edn, Verlag Chemie, Weinheim (Bergstrasse), Germany
23 Bernardi, P., Scorrano, L., Colonna, R., Petronilli, V. and di Lisa, F. (1999) Mitochondria and cell death. Mechanistic aspects and methodological issues. Eur. J. Biochem. **264**, 687–701
24 Floryk, D. and Houstek, J. (1999) Tetramethyl rhodamine methyl ester (TMRM) is suitable for cytofluorometric measurements of mitochondrial membrane potential in cells treated with digitonin. Biosci. Rep. **19**, 27–34
25 Gnaiger, E., Kuznetsov, A., Lassnig, B., Fuchs, A., Reck, M., Renner, K., Stadlmann, S., Rieger, G. and Margreiter, R. (1998) High Resolution Respirometry – Optimum Permeabilization of the Cell Membrane by Digitonin, Chalmers Reproservice, Gothenburg
26 Renner, K., Amberger, A., Konwalinka, G., Kofler, R. and Gnaiger, E. (2003) Changes of mitochondrial respiration, mitochondrial content and cell size after induction of apoptosis in leukemia cells. Biochim. Biophys. Acta **1642**, 115–123
27 Steinlechner-Maran, R., Eberl, T., Kunc, M., Margreiter, R. and Gnaiger, E. (1996) Oxygen dependence of respiration in coupled and uncoupled endothelial cells. Am. J. Physiol. **271**, C2053–C2061
28 Stein, G. H. and Dulic, V. (1995) Origins of G(1) arrest in senescent human fibroblasts. Bioessays **17**, 537–543
29 Susin, S. A., Lorenzo, H. K., Zamzami, N., Marzo, I., Snow, B. E., Brothers, G. M., Mangion, J., Jacotot, E., Costantini, P., Loeffler, M. et al. (1999) Molecular characterization of mitochondrial apoptosis-inducing factor. Nature (London) **397**, 441–446
30 Zhou, Y. T., Shimabukuro, M., Koyama, K., Lee, Y., Wang, M. Y., Trieu, F., Newgard, C. B. and Unger, R. H. (1997) Induction by leptin of uncoupling protein-2 and enzymes of fatty acid oxidation. Proc. Natl. Acad. Sci. U.S.A. **94**, 6386–6390
31 Fukami, J., Anno, K., Ueda, K., Takahashi, T. and Ide, T. (1995) Enhanced expression of cyclin D1 in senescent human fibroblasts. Mech. Ageing Dev. **81**, 139–157
32 Mathur, A., Hong, Y., Kemp, B. K., Barrientos, A. A. and Erusalimsky, J. D. (2000) Evaluation of fluorescent dyes for the detection of mitochondrial membrane potential changes in cultured cardiomyocytes. Cardiovasc. Res. **46**, 126–138
33 Gnaiger, E., Rieger, G., Kuznetsov, A., Fuchs, A., Stadlmann, S., Lassnig, B., Hengster, P., Eberl, T. and Margreiter, R. (1997) Mitochondrial ischemia-reoxygenation injury and plasma membrane integrity in human endothelial cells. Transplant. Proc. **29**, 3524–3526
34 Stadlmann, S., Rieger, G., Amberger, A., Kuznetsov, A. V., Margreiter, R. and Gnaiger, E. (2002) H_2O_2-mediated oxidative stress versus cold ischemia-reperfusion: mitochondrial respiratory defects in cultured human endothelial cells. Transplantation **74**, 1800–1803
35 Rolfe, D. F. and Brown, G. C. (1997) Cellular energy utilization and molecular origin of standard metabolic rate in mammals. Physiol. Rev. **77**, 731–758
36 Goldstein, S., Ballantyne, S. R., Robson, A. L. and Moerman, E. J. (1982) Energy metabolism in cultured human fibroblasts during aging *in vitro*. J. Cell Physiol. **112**, 419–424
37 Wang, W., Yang, X., Lopez De Silanes, I., Carling, D. and Gorospe, M. (2003) Increased AMP:ATP ratio and AMP-activated kinase activity during cellular senescence linked to reduced HuR function. J. Biol. Chem. **278**, 27016–27023
38 Yan, L. J. and Sohal, R. S. (1998) Mitochondrial adenine nucleotide translocase is modified oxidatively during aging. Proc. Natl. Acad. Sci. U.S.A. **95**, 12896–12901

39 Petronilli, V., Costantini, P., Scorrano, L., Colonna, R., Passamonti, S. and Bernardi, P. (1994) The voltage sensor of the mitochondrial permeability transition pore is tuned by the oxidation–reduction state of vicinal thiols. Increase of the gating potential by oxidants and its reversal by reducing agents. J. Biol. Chem. **269**, 16638–16642
40 Mather, M. and Rottenberg, H. (2000) Aging enhances the activation of the permeability transition pore in mitochondria. Biochem. Biophys. Res. Commun. **273**, 603–608
41 Kokoszka, J. E., Coskun, P., Esposito, L. A. and Wallace, D. C. (2001) Increased mitochondrial oxidative stress in the Sod2 (+/−) mouse results in the age-related decline of mitochondrial function culminating in increased apoptosis. Proc. Natl. Acad. Sci. U.S.A. **98**, 2278–2283
42 Martinez, A. O., Over, D., Armstrong, L. S., Manzano, L., Taylor, R. and Chambers, J. (1991) Separation of two subpopulations of old human fibroblasts by mitochondria (rhodamine 123) fluorescence. Growth Dev. Aging **55**, 185–191
43 Goldstein, S., Moerman, E. J. and Porter, K. (1984) High-voltage electron microscopy of human diploid fibroblasts during ageing *in vitro*. Morphometric analysis of mitochondria. Exp. Cell Res. **154**, 101–111
44 Dulloo, A. G. and Samec, S. (2001) Uncoupling proteins: their roles in adaptive thermogenesis and substrate metabolism reconsidered. Br. J. Nutr. **86**, 123–139
45 Echtay, K. S., Murphy, M. P., Smith, R. A., Talbot, D. A. and Brand, M. D. (2002) Superoxide activates mitochondrial uncoupling protein 2 from the matrix side. Studies using targeted antioxidants. J. Biol. Chem. **277**, 47129–47135
46 Goldstein, S. and Korczack, L. B. (1981) Status of mitochondria in living human fibroblasts during growth and senescence *in vitro*: use of the laser dye rhodamine 123. J. Cell Biol. **91**, 392–398
47 Salvioli, S., Ardizzoni, A., Franceschi, C. and Cossarizza, A. (1997) JC-1, but not DiOC6(3) or rhodamine 123, is a reliable fluorescent probe to assess $\Delta\psi$ changes in intact cells: implications for studies on mitochondrial functionality during apoptosis. FEBS Lett. **411**, 77–82
48 Martinez, A. O., Vigil, A. and Vila, J. C. (1986) Flow-cytometric analysis of mitochondria-associated fluorescence in young and old human fibroblasts. Exp. Cell Res. **164**, 551–555
49 Martinez, A. O., Vara, C. and Castro, J. (1987) Increased uptake and retention of rhodamine 123 by mitochondria of old human fibroblasts. Mech. Ageing Dev. **39**, 1–9
50 Greco, M., Villani, G., Mazzucchelli, F., Bresolin, N., Papa, S. and Attardi, G. (2003) Marked aging-related decline in efficiency of oxidative phosphorylation in human skin fibroblasts. FASEB J. **17**, 1706–1708

Received 16 January 2004/5 March 2004; accepted 12 March 2004
Published as BJ Immediate Publication 12 March 2004, DOI 10.1042/BJ20040095